

Characterization of Real-time Haptic Feedback from Multimodal Neural Network-based Force Estimates during Teleoperation

Zonghe Chua¹, *Student Member, IEEE* and Allison M. Okamura¹, *Fellow, IEEE*

Abstract—Force estimation using neural networks is a promising approach to enable haptic feedback in minimally invasive surgical robots without end-effector force sensors. Various network architectures have been proposed, but none have been tested in real-time with surgical-like manipulations. Thus, questions remain about the real-time transparency and stability of force feedback from neural network-based force estimates. We characterize the real-time impedance transparency and stability of force feedback rendered on a da Vinci Research Kit teleoperated surgical robot using neural networks with vision-only, state-only, or state and vision inputs. Networks were trained on an existing dataset of teleoperated manipulations without force feedback. We measured real-time transparency without rendered force feedback by commanding the patient-side robot to perform vertical retractions and palpations on artificial silicone tissue. To measure stability and transparency during teleoperation with force feedback to the operator, we modeled a one-degree-of-freedom human and surgeon-side manipulandum that moved the patient-side robot to perform manipulations. We found that the multimodal vision and state network displayed more transparent impedance than single-modality networks under no force feedback. State-based networks displayed instabilities during manipulation with force feedback. This instability was reduced in the multimodal network when refit with additional data collected during teleoperation with force feedback.

I. INTRODUCTION

Safe tissue handling is an important and often evaluated component of human skill for robot-assisted minimally invasive surgery (RMIS) [1][2]. However, it is thought to be a difficult skill to develop due to the lack of haptic feedback in teleoperated RMIS platforms. Displaying kinesthetic force feedback to the surgeon is one way to overcome this limitation. This typically requires three-degree-of-freedom force sensing at the tip of the robot end-effector with forces displayed to the teleoperator at high update rates. It is difficult to achieve this cost-effectively in RMIS due to the small size of the surgical manipulators and requirements for biocompatibility and sterilizability [3].

To circumvent direct force sensing, force estimation through physics-based dynamic models that use robot kinematic and dynamic state inputs have been explored [4]–[6], though they have difficulty accurately estimating external joint torques in the most distal degrees of freedom, especially outside the range of joint angles and velocities used to fit their parameters. Vision-based methods that try to estimate interaction force from environmental deformation have also

been explored through the use of stereo image reconstruction and finite-element mesh fitting, with the limitation being that these models are computationally expensive and highly sensitive to the definition of the mesh anchors [7].

Neural networks represent a promising approach to force estimation, replacing the need for explicit model specification with the need for more data. This approach has been used to model the dynamics of the robot in free space to predict external joint torques during environment interaction using only robot state inputs through supervised [8] or self-supervised learning [9]. Other methods attempt to use both vision- and state-based inputs to estimate forces, with many architectures also incorporating sequential temporal inputs either through recurrent neural networks [10]–[12] or a transformer network [13]. Our prior work has shown that static image and robot state-based models that do not encode temporal history can also estimate forces with similar accuracy, with the added benefit of faster computation time [14]. Deep learning approaches resulted in good offline accuracy relative to physics-based dynamic models, making them promising for applications such as offline surgical skill evaluation. However, with the exception of Tran et al. who conducted a pilot stiffness discrimination study with force feedback from a neural network [8], these methods have never been evaluated in real-time teleoperation. Thus, questions remain about their real-time performance in terms of impedance transparency, and human-in-the-loop stability.

In this work, we characterize the impedance transparency and stability of force estimation neural networks, through two experiments using neural networks with either robot state-only, vision-only, or multimodal (vision and robot state) inputs from a single time point that output an end-effector force estimate in the three Cartesian directions. In the first experiment, which we define as *stiffness estimation during open-loop manipulation*, we characterize the impedance transparency of force estimation when the patient-side manipulator (PSM) follows commanded trajectories to perform unidirectional stiffness estimation. This enabled us to quantify the real-time performance of networks in the absence of closed-loop dynamics that could affect transparency.

In the second experiment, which we define as *closed-loop force feedback manipulation*, we characterize impedance transparency and stability when a one-degree-of-freedom model of the human teleoperator and surgeon-side manipulandum (SSM) moves the PSM to perform tissue manipulations in each of the Cartesian directions, thus mimicking bilateral teleoperation. As a baseline comparison, we used force estimates from a physics-based dynamic model and

*This work was supported by a Stanford Bio-X Fellowship.

¹Z. Chua and A. M. Okamura are with the Mechanical Engineering Department, Stanford University, CA 94305, USA. chuazh@stanford.edu, aokamura@stanford.edu

the ground truth interaction force as measured by a force sensor placed underneath the artificial tissue.

Given the observed impedance transparency and stability behavior of the multimodal network during the closed-loop force feedback manipulation experiment, we attempted to improve performance by refitting the network parameters with additional data from teleoperation with force feedback from the neural network. We compare this approach to refitting with additional data collected under no force feedback, and from teleoperation with ideal force feedback from a force sensor. Lastly, we present a demonstration of teleoperation with force feedback using estimates from the refit neural network.

II. METHODS

A. Hardware Setup

A da Vinci Research Kit (dVRK) right PSM [15], a stereo camera assembly, and a custom artificial tissue mounting platform (Fig. 1) were used for all experiments. In addition, the dVRK right SSM was also used when actual teleoperation was required. The stereo camera assembly consisted of two cameras (Flea3, FLIR Systems, Wilsonville, OR, USA) that captured 960×540 images at 30 Hz. On this platform, a piece of artificial tissue (Professional Skin Pad Mk1, Limbs & Things, Savannah, GA, USA) measuring $125 \times 72 \times 3$ mm, with the silicone layer separated from the sponge layer, was clamped to a rigid base with a 6-axis force-torque sensor (Nano17, ATI Industrial Automation, Apex, NC, USA) mounted beneath. To ensure a tissue-like border around the manipulated artificial tissue, the same silicone material was clamped to the top and bottom border of the tissue. A Cadere forceps tool was mounted on the PSM. Relative to the platform center, the PSM base frame was positioned 14.5 cm to the right. The camera was positioned such that the left camera was centered on the middle of the tissue and its field of view cropped to 300×300 before being resized to 224×224 for input to the vision-based networks.

Control of the robot, sensor output processing, and dynamics simulation were split between two computers networked through Robot Operating System (ROS). The first computer handled the dVRK low-level control, robot state sensing, and force sensing processes at 1000 Hz. The second computer ran the image processing, dynamics simulation, force estimation, and high-level arm trajectory command processes.

B. Network and Model Architecture

The force estimation neural networks used either state-only (S), vision-only (V), or vision and state (VS) inputs with parameters fit from a dataset of teleoperated manipulations on artificial tissue performed with no force feedback to the human operator as described in [14]. The S network was a fully connected network with 6 layers of sizes 500, 1000×3 , 500, and 50, respectively. The V network was a ResNet50 [16] architecture, while the VS network compressed the encoded output of a ResNet50 network to a 30-dimensional vector and concatenated it with the robot state input before passing it through three fully connected layers of size 84,

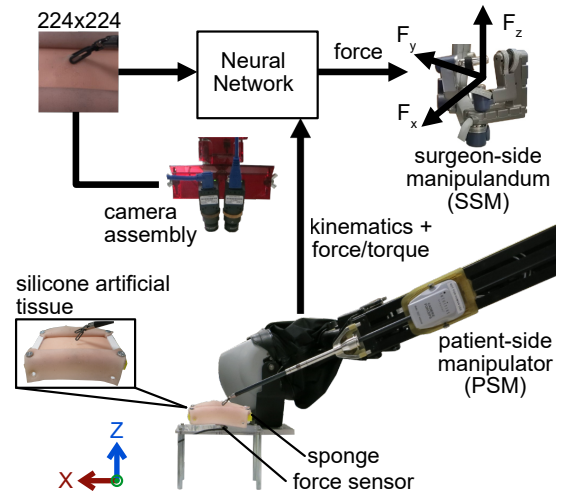


Fig. 1. Experimental set up comprising a da Vinci Research Kit equipped with Cadere forceps and silicone artificial tissue. Neural network architectures that use either image or robot state inputs, or a combination of both, were used to estimate interaction forces and render haptic feedback.

180, and 50, respectively. In all networks, the final output was a force estimate in the three Cartesian dimensions. Vision inputs were RGB monocular images of size $224 \times 224 \times 3$, while state inputs were 54-dimensional vectors composed of robot joint positions, velocities, and torques, and Cartesian position, velocity, and force. All image inputs were normalized by the ImageNet [17] mean and standard deviation, while the state inputs were normalized by the mean and standard deviation of the training data set.

A physics-based dynamic model [6], henceforth denoted as D, was used as a baseline force estimation model. We performed parameter estimation using the methods from [6] and subtracted the estimated joint torques from the measured joint torques to obtain the interaction joint torques. The interaction torques were multiplied with the pseudoinverse of the Jacobian transpose to arrive at the estimated interaction forces at the end-effector. In all experiments, the estimated forces from D were low-pass filtered at a cutoff of 1 Hz. This low cutoff was required to reduce the force oscillations that induced large movement oscillations during the closed-loop force feedback manipulation experiment. Without filtering, the manipulated silicone would slip out of grasp resulting in failed experiments. For ground truth comparison, we used forces measured through a force sensor sampled at 1000 Hz. This method will be denoted as FS.

C. Stiffness Estimation during Open-loop Manipulation

To characterize the material impedance that would be estimated by the force estimation methods in real-time during open-loop (no direct force feedback) manipulation, the PSM was programmed to autonomously perform vertical palpations and retractions, which are common probing actions used during surgery to judge tissue characteristics. The palpation movement was performed by commanding the PSM to track 1 s minimum jerk trajectories [18] for loading and unloading in the z-direction with a peak displacement

TABLE I
NUMBER OF EXAMPLES USED TO FIT AND VALIDATE EACH MODEL

Dataset Teleoperation Condition	Train	Validation
Original dataset C configuration [14]	14020	7036
No force feedback (VS-NF)	14380	7192
Force feedback from force sensor (VS-FS)	14379	7192
Force feedback from neural network (VS-EF)	14385	7194

from the grasp. For manipulations in the x- and y-directions, the material was further pre-tensioned in the z-direction by 1 N. Then a sequence of minimum jerk trajectories were commanded to the human plant, first by +75 mm in 1 s, then by -150 mm in 2 s, +150 mm in 2 s, -150 mm in 2 s before returning to the pre-tensioned position by moving +75 mm in 1 s. Between each movement, the position was held for 2 s. These movements, when scaled by the 0.2 scaling factor, are equivalent to ideal displacements of the PSM by 15 mm or 30 mm (Fig. 2c). For the z-direction manipulations, there was no pre-tensioning. This allowed the commanded manipulations to cover both compression and tension regimes. Instead, the same minimum jerk trajectories were commanded with the final movement returning the PSM to the initial force-neutral position (Fig. 2c).

To quantify impedance transparency during the manipulations, the root mean squared error (RMSE) of the estimated force with respect to the ground truth force was used. To quantify the stability of the system with closed-loop force feedback, a passivity-based approach was adopted. The complex dynamics of the robot, coupled with the non-dynamical multimodal input-output formulation of the neural networks, and their black-box nature, makes Lyapunov analysis intractable.

The passivity-based analysis was performed by implementing a passivity observer and controller on the SSM-side and measuring the root mean square (RMS) control effort produced by the passivity controller in its attempt to passivate the system. A windowed passivity observer was implemented such that the windowed energy observed at the SSM on the N^{th} time step is

$$E_{\text{win}}(N) = \sum_{n=N-k+1}^N F_{\text{feedback}}(n) \dot{x}(n) \Delta t \quad (3)$$

where $k = 10$ is the sampling window size and Δt the period between the n^{th} and the $(n-1)^{\text{th}}$ measurement [20]. k was tuned empirically so that the controller could react quickly to negative energy production as opposed to storing energy and only going negative after a period of negative energy was produced. A passivity controller [21] was used to generate the passivating control force using the control rule

$$F_{\text{passive}}(n) = \begin{cases} -\dot{x} \frac{E_{\text{win}}(n)}{\dot{x}^2 \Delta t} & \text{if } E_{\text{win}}(n) < 0 \\ 0 & \text{otherwise} \end{cases} \quad (4)$$

where the variable damping term $\frac{E_{\text{win}}(n)}{\dot{x}^2 \Delta t}$ was limited to a maximum value of 250 N s m^{-1} . The combined passivity

controller and observer module was run at 1000 Hz.

For each type of force estimation method with and without the passivity module, the trajectory sequence for each Cartesian direction was performed three times on three different silicone samples with the order of estimation method and passivity condition (with and without the passivity module) randomized. The displacement of the robot end-effector was measured via its joint encoders.

E. Refitting Network Parameters with Teleoperated Force Feedback Data

The addition of the human and SSM into the control loop results in altered dynamics and prediction errors that are not observed by the neural networks during training. Thus, additional data under the new dynamics can likely be used to further improve the network performance. To test the effect of refitting the neural networks with additional data collected from teleoperation with force feedback from a trained neural network, we collected training and validation examples in three different conditions: Teleoperation without force feedback (VS-NF), teleoperation with force feedback from a force sensor (VS-FS), and teleoperation with estimated force feedback from the original VS network (VS-EF). Training a network with data collected under no force feedback controls for the possibility that refitting with more data under no force feedback would lead to improved performance. Similarly, training a network on additional data that used force sensor feedback enabled us to compare performance against a network that was trained on movements performed under conditions of ideal force feedback.

The movements performed during data collection were similar to the trajectories generated in the closed-loop force feedback manipulation experiment. They consisted of slow palpations and retractions that were held static for a period of time, as opposed to the brief palpations and retractions found in the original training dataset. To ensure that the contribution of the new data had equal influence on the parameter fitting process as the original data, we took only a subset of the original data to ensure an approximately equal amount of original and new training examples. This consisted of the center (C) position training examples from the original dataset as shown in Fig. 1 of [14] because this was the same condition that was being evaluated in the closed-loop force feedback manipulation experiments. The number of examples for each condition is shown in Table I.

Three new networks, VS-NF, VS-FS, and VS-EF were trained from the default scratch initialization of VS from [14] on the augmented dataset for 50 epochs at a learning rate of 0.001 and an L1 regularization of 0.001 using Adam [22]. Each network was then used to perform the closed-loop force feedback manipulation experiments as described in Sec. II-D.

F. Demonstration of Teleoperation with Force Feedback

In our experiments, the VS-EF network exhibited the best transparency and stability characteristics overall. To demonstrate the performance of the network under actual

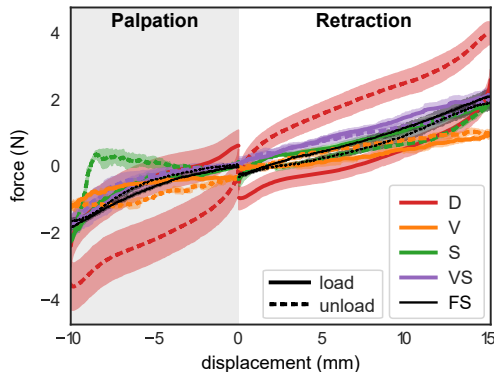


Fig. 4. Average force-displacement curves (estimated stiffness) during z-direction palpation and retraction maneuvers from three materials. Shaded regions denote ± 1 standard deviation.

teleoperation, a human teleoperated the SSM with force feedback. They performed a series of slow and fast palpations and retractions on the artificial tissue in the three Cartesian degrees-of-freedom over 35 s, with the VS-EF network running at 60 Hz.

III. RESULTS AND DISCUSSION

A. Stiffness Estimation during Open-loop Manipulation

For the different force estimation methods, the force estimates over the range of palpation and retraction displacements were averaged over the three movement cycles for each material. The resultant material force-displacement curves were then averaged to derive the average stiffness curve of the artificial tissue as estimated by each force estimation method (Fig. 4).

The multimodal VS network achieved the closest replication of the ground truth stiffness of the artificial tissue and possessed some of the advantages and limitations of each single-modality network. Based on the shapes of the stiffness curves in Fig. 4, the VS and S networks, which used state inputs, better captured the impedance of the artificial tissue compared to V and D. While D managed to capture the trend of increasing stiffness as displacement increases, it overestimated the forces during the unloading phase of the maneuvers. Due to the delay introduced by low-pass filtering, D estimated unloading forces that were higher than in loading. V was unable to capture the increasing stiffness as displacement increased. This was likely due to the diminishing amount of visual force information provided by the environment as stiffness increased. Despite the lack of temporal information encoded in its inputs, V estimated higher unloading forces relative to loading, though this difference was not as pronounced as in D.

While VS and S performed similarly in retraction, S rendered very high stiffness during unloading in palpation resulting in the rendered force dropping quickly to zero and then going in the opposite direction. As noted in [14], state inputs can create a tendency to overfit in the z-direction due to a reduced amount of variation of the tissue location in that direction in the training dataset. Given that

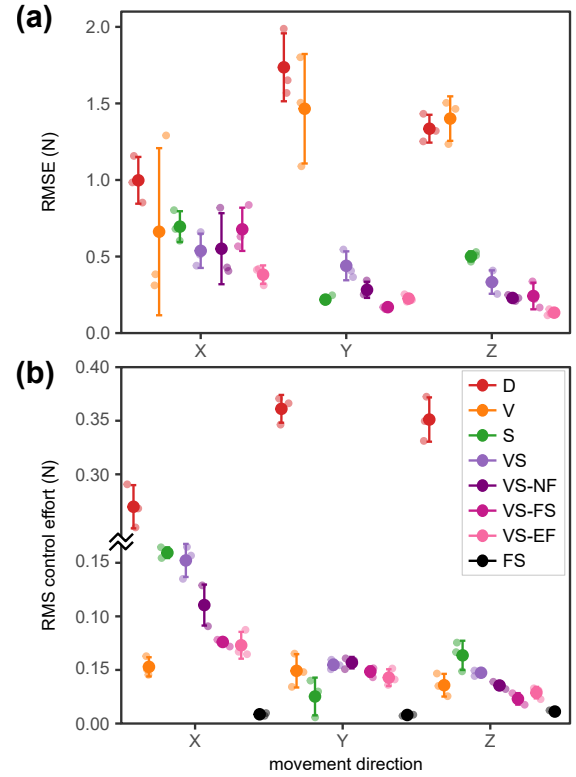


Fig. 5. (a) Root mean squared error of the estimated force feedback compared to the ground truth force measurement, and (b) root mean square passivating control effort during periods when the target position was held by the human-manipulandum model for each Cartesian direction, averaged over three different materials. Error bars denote ± 1 standard deviation.

V has documented robustness to changing viewpoints [14], the contribution of vision inputs also likely helped reduce overfitting in VS.

The vision-based networks produced a force bias in either palpation, as seen in the force estimated for V, or in retraction as seen for VS (Fig. 4). This suggests that there are visual uncertainties at small displacements, such as if the manipulator is in contact with the environment, or if the material is slipping from grasp, that could have confounded the force estimates that are dependent on vision inputs.

B. One-degree-of-freedom Closed-loop Force Feedback Manipulation with Modeled Teleoperation Dynamics

To quantify impedance transparency during the execution of the movements, we used the RMSE of the estimated force feedback with respect to the ground truth measurement (Fig. 5a). In the x- and z-directions, among the models fit using the original dataset, the VS networks produced the lowest RMSE when used for force feedback in teleoperation. In the y-direction, the S network force feedback resulted in the lowest RMSE. However, the RMSE values for VS in the x-, y- and z-directions of 0.534, 0.439, and 0.331 are higher than those in the test dataset from [14], which were 0.300, 0.374, and 0.278 respectively. For the S network the RMSE values in the x- and z-directions of 0.695, and 0.501 are higher than those in for the test dataset from [14], which

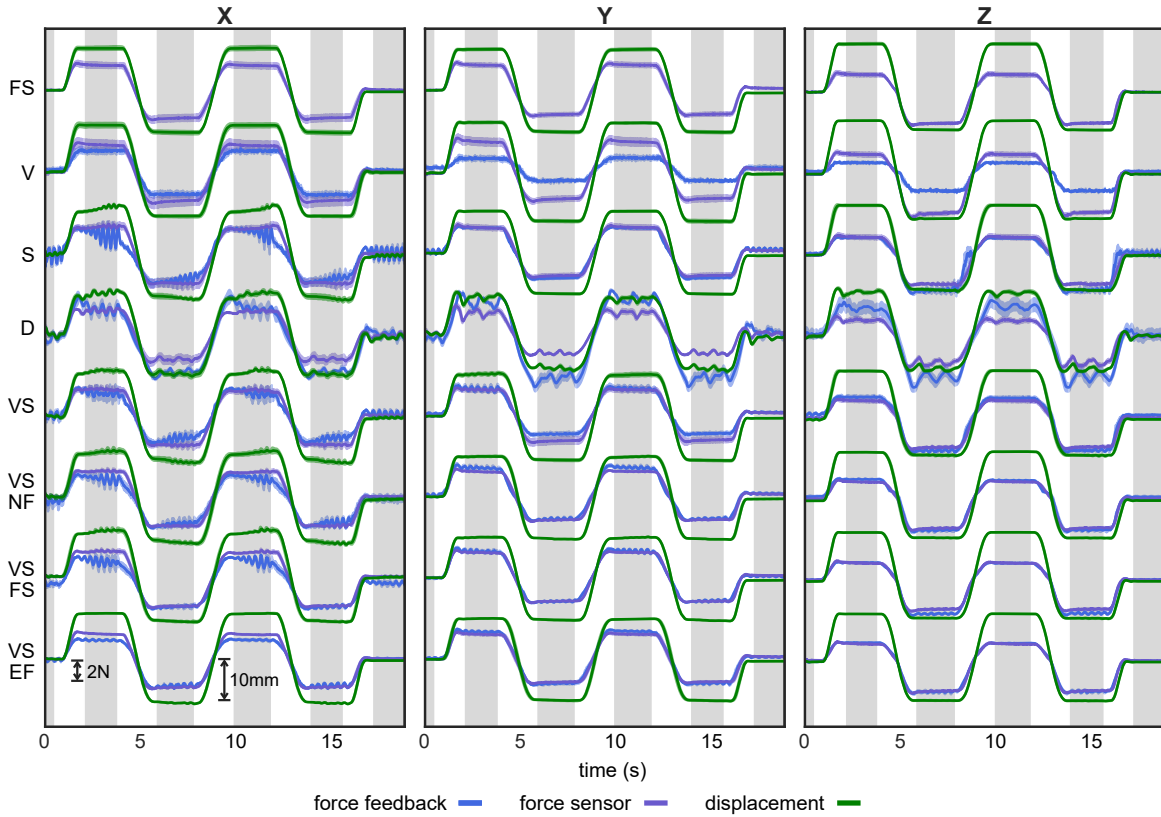


Fig. 6. Force feedback, ground truth force sensor measurement and displacement over time for each force estimation method. For the FS method, the force sensor measurement is also used for force feedback. Shaded regions denote ± 1 standard deviation. Grey areas denote the periods where the human-manipulandum model was attempting to hold a position.

were 0.316, and 0.326 respectively. These larger RMSE values stem from force oscillations induced by the closed-loop system when the human-SSM model was attempting to hold a position (Fig. 6). In the y-direction, the difference in RMSE between the VS and S network can be explained by the force oscillations induced in the VS network and not in the S network.

In the y- and z-directions, using V for force feedback results in poor transparency as measured by RMSE (Fig. 5). As observed in the stiffness estimation during open-loop manipulation experiments, there was poor transparency rendered by V in the z-direction during palpation, where there is a lack of visual force information at high displacements (Fig. 6). In the y-direction, the high RMSE was likely due to the lack of depth perception in that direction as the network relies only on a monocular image.

Enforcing the passivity condition on the SSM is a very conservative stabilization method that results in passivating force being applied any time the material is being unloaded. Thus, to quantify stability when the system was in an unstable state and not just temporarily active, we only considered passivating control effort during portions of time where the human-SSM model was attempting to hold a position. The time periods were calculated by detecting movement onset and offset via the velocity profile from the unpassivated movements in the FS condition. These periods

are highlighted in grey in Fig. 6. The passivation effort for all methods were low-pass filtered at 100 Hz, and the average RMS passivating control effort for each condition for each Cartesian direction presented in Fig. 5b. Due to the force and displacement oscillation in S and VS for the x- and z-directions, high RMS passivating control effort was produced by the passivity controller for those networks compared to V. Due to the lack of induced oscillations in the y-direction for V and S, we see that their resultant RMS passivating control efforts were less compared to VS.

One method to reduce these unstable oscillations is to filter the force feedback. Upon inspection of the frequency spectrum of the detrended forces during periods when the human-SSM model was attempting to hold a position, it can be seen that the frequencies of the force oscillations in x- and z-direction are in the range of 3-5 Hz (Fig. 7), which is in the range of frequencies of human volitional movement. This result implies that using filtering at the target cutoff frequency as a strategy to attenuate oscillatory forces would significantly reduce impedance transparency.

C. Refitting Network Parameters with Teleoperated Force Feedback Data

Among the refitted models, refitting with data from teleoperation with closed-loop force feedback (VS-FS and VS-EF) overall resulted in better transparency and stability behavior

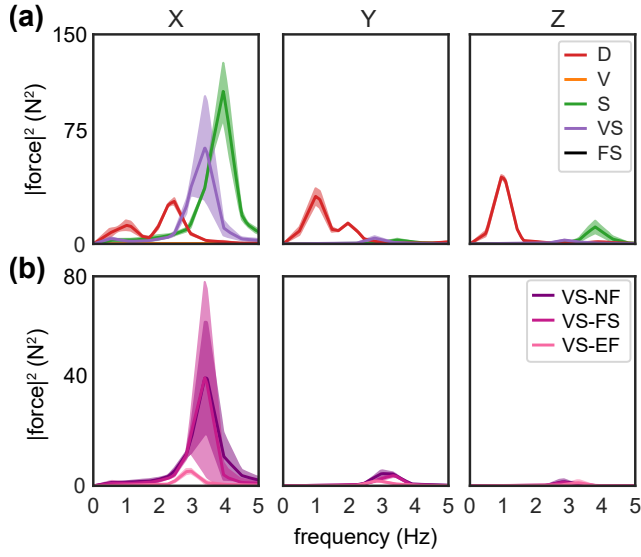


Fig. 7. Frequency spectrum of detrended force in the closed-loop force feedback manipulation experiments during periods when the human-manipulandum model was attempting to hold a position averaged over three artificial tissue samples for the: (a) Original force estimation methods, and (b) VS neural networks refit with newly collected data from different teleoperation conditions. Shaded regions denote ± 1 standard deviation.

across directions than refitting with data from teleoperation with no force feedback (VS-NF). Across all directions, refitting with the new data resulted in lower RMSE compared to the original VS network except in the case of VS-FS in the x-direction (Fig. 5a). The lower error from the refitted models is expected as the data used for refitting was collected under operating conditions that more closely resembled that of the experiment. RMSE was lower in both VS-FS and VS-EF compared to VS-NF in the y- and z-directions, while VS-EF had lower RMSE compared to VS-NF in x (Fig. 5a). VS-EF had lower RMSE than VS-FS in x and z.

In all directions, VS-FS and VS-EF required less passivating control effort compared to VS-NF. In the x- and y- directions, VS-EF required less passivating control effort compare to VS-FS (Fig 5b). However, the difference in passivating control effort between VS-FS and VS-EF are not pronounced, as there is a point where the force oscillations are small enough to be significantly damped out by the human plant and hence fail to induce much oscillatory movement. The trends in RMSE and RMS control effort are reflected in Fig. 6 as smaller force and displacement oscillations for VS-FS and VS-EF compared to VS-NF, and in Fig. 7b as the attenuation of the frequency peaks in the x- and y- direction for VS-EF.

By comparing the ground truth measurement against the force feedback from the estimates for the original S and VS networks in Fig. 6, we see that a chief contributor of the poor transparency is the overestimation of the force during the oscillatory movements. Thus, by refitting to data that captures these prediction errors, the error was likely reduced. With the lower oscillatory forces, oscillatory movements are damped out or eliminated, thus improving the stability

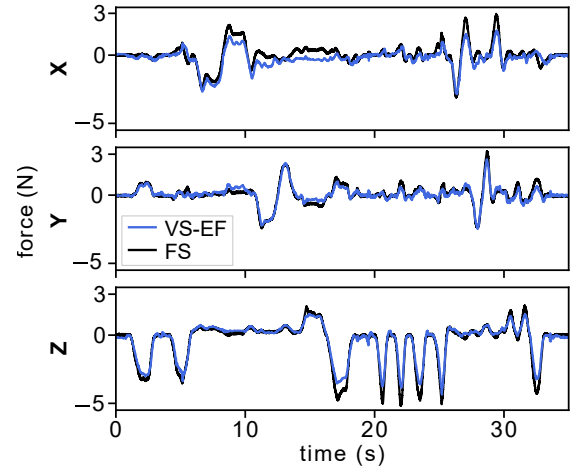


Fig. 8. Force feedback displayed to the human teleoperator based on estimates from the VS-EF network against the ground truth measurement from the force sensor during manipulation of artificial tissue.

behavior of the system. This approach is similar to methods from neuro-adaptive control [23][24] that iteratively update their parameters with the availability of more data, with the difference being that they do so online, as opposed to offline, in a stability-preserving manner.

D. Demonstration of Teleoperation with Force Feedback

The demonstration of human teleoperation with force feedback from the VS-EF network started with a palpation in z, followed by slow movements with holds in the x-y-, and z-directions within the first twenty seconds. In x, the hold at 8.5s showed small force oscillations in the positive x-direction, which is in agreement with the behavior seen in closed-loop force feedback manipulation with modeled human-SSM dynamics. However, the force oscillations in z and y were not noticeable.

IV. CONCLUSION

Our work characterized the quality of open- and closed-loop force feedback using neural networks during teleoperation of a dVRK in terms of impedance transparency and stability behavior via passivity concepts. We showed that a vision-only network displayed poor transparency during high stiffness interactions and in directions with low depth perception, while state-based networks were susceptible to oscillatory forces that could result in instability. The oscillatory forces were minimized through refitting with additional data from teleoperation with force feedback. Of the types of force feedback used during the collection of additional data, using estimated force from the neural network resulted in the most consistent improvements in transparency and stability behavior.

In this work, only a single robot starting configuration was used for the experiments. In different configurations, the robot would rely on various joints for achieving movement in the task space to different extents. Such a difference in configuration could potentially result in different close-looped system behavior. Thus, future work will quantify the

transparency and stability behavior of the system in different configurations.

The V network showed no tendency to induce unstable oscillations during teleoperation with force feedback despite being only run at 60Hz. This reduction in force oscillations was also seen in the VS network after refitting with additional data from teleoperation with force feedback and suggests that instability was not due to low update rates. This could be due to the fact that the artificial tissue had low stiffness and high damping such that the low update rate did not result in instability [25]. The stability at high stiffness can be explored further in use cases that contain stiff interactions like knot tying.

Because the VS network was shown to have the best open-loop impedance transparency and also displayed improved performance after refitting with data from teleoperation with force feedback, methods should be explored to further improve its performance. One promising line of work is to continue iteratively with the data collection and the offline refitting process to verify if the oscillatory forces can be eliminated entirely.

While the multimodal inputs and formulation of the neural network input-output as a non-dynamical system make it difficult to formulate stability guarantees, the methods presented here are shown to be capable of providing real-time force feedback that can be made stable in controlled and structured environments. Thus these methods can potentially be used to provide force feedback in non-safety-critical settings with consistent environments such as in surgical training. Such an application is particularly promising in the light of recent work that has explored how training in teleoperation with force information can lead to better performance in conditions where there is none [26].

V. ACKNOWLEDGMENTS

The authors would like to thank Anton Deguet for his help with dVRK control, and Negin Heravi and Anthony Jarc for their advice on neural network training.

REFERENCES

- [1] A. C. Goh, D. W. Goldfarb, J. C. Sander, B. J. Miles, and B. J. Dunkin, "Global evaluative assessment of robotic skills: Validation of a clinical assessment tool to measure robotic surgical skills," *The Journal of Urology*, vol. 187, no. 1, pp. 247–252, 2012.
- [2] J. Martin, G. Regehr, R. Reznick, H. Macrae, J. Murnaghan, C. Hutchison, and M. Brown, "Objective structured assessment of technical skill (OSATS) for surgical residents," *British Journal of Surgery*, vol. 84, no. 2, pp. 273–278, 1997.
- [3] N. Enayati, E. De Momi, and G. Ferrigno, "Haptics in robot-assisted surgery: Challenges and benefits," *IEEE Reviews in Biomedical Engineering*, vol. 9, pp. 49–65, 2016.
- [4] G. A. Fontanelli, F. Ficuciello, L. Villani, and B. Siciliano, "Modelling and identification of the da Vinci Research Kit robotic arms," in *IEEE/RSJ International Conference on Intelligent Robots and Systems*, 2017, pp. 1464–1469.
- [5] F. Piqué, M. N. Boushaki, M. Brancadoro, E. De Momi, and A. Menciassi, "Dynamic modeling of the da Vinci Research Kit arm for the estimation of interaction wrench," in *International Symposium on Medical Robotics*, 2019, pp. 1–7.
- [6] Y. Wang, R. Gondokaryono, A. Munawar, and G. S. Fischer, "A convex optimization-based dynamic model identification package for the da Vinci Research Kit," *IEEE Robotics and Automation Letters*, vol. 4, no. 4, pp. 3657–3664, 2019.
- [7] N. Haouchine, W. Kuang, S. Cotin, and M. Yip, "Vision-based force feedback estimation for robot-assisted surgery using instrument-constrained biomechanical three-dimensional maps," *IEEE Robotics and Automation Letters*, vol. 3, no. 3, pp. 2160–2165, 2018.
- [8] N. Tran, J. Y. Wu, A. Deguet, and P. Kazanzides, "A deep learning approach to intrinsic force sensing on the da Vinci surgical robot," in *4th IEEE International Conference on Robotic Computing*, 2020, pp. 25–32.
- [9] N. Yilmaz, J. Y. Wu, P. Kazanzides, and U. Tumerdem, "Neural network based inverse dynamics identification and external force estimation on the da Vinci Research Kit," in *IEEE International Conference on Robotics and Automation*, 2020, pp. 1387–1393.
- [10] A. I. Aviles, S. M. Alsaleh, J. K. Hahn, and A. Casals, "Towards retrieving force feedback in robotic-assisted surgery: A supervised neuro-recurrent-vision approach," *IEEE Transactions on Haptics*, vol. 10, no. 3, pp. 431–443, 2016.
- [11] A. Marban, V. Srinivasan, W. Samek, J. Fernandez, and A. Casals, "Estimation of interaction forces in robotic surgery using a semi-supervised deep neural network model," in *IEEE International Conference on Intelligent Robots and Systems*, 2018, pp. 761–768.
- [12] A. Marban, V. Srinivasan, W. Samek, J. Fernández, and A. Casals, "A recurrent convolutional neural network approach for sensorless force estimation in robotic surgery," *Biomedical Signal Processing and Control*, vol. 50, pp. 134–150, 2019.
- [13] H. Shin, H. Cho, D. K. Ko, S. C. Lim, and W. Hwang, "Sequential image-based attention network for inferring force estimation without haptic sensor," *IEEE Access*, vol. 7, pp. 150 237–150 246, 2019.
- [14] Z. Chua, A. M. Jarc, and A. M. Okamura, "Toward force estimation in robot-assisted surgery using deep learning with vision and robot state," in *IEEE International Conference on Robotics and Automation*, 2021, arXiv:2011.02112.
- [15] P. Kazanzides, Z. Chen, A. Deguet, G. S. Fischer, R. H. Taylor, and S. P. DiMaio, "An open-source research kit for the da Vinci Surgical System," in *IEEE International Conference on Robotics and Automation*, 2014, pp. 6434–6439.
- [16] K. He, X. Zhang, S. Ren, and J. Sun, "Deep residual learning for image recognition," in *IEEE Conference on Computer Vision and Pattern Recognition*, 2016, pp. 770–778.
- [17] J. Deng, W. Dong, R. Socher, L.-J. Li, K. Li, and L. Fei-Fei, "Imagenet: A large-scale hierarchical image database," in *IEEE Conference on Computer Vision and Pattern Recognition*, 2009, pp. 248–255.
- [18] T. Flash and N. Hogan, "The coordination of arm movements: An experimentally confirmed mathematical model," *Journal of Neuroscience*, vol. 5, no. 7, pp. 1688–1703, 1985.
- [19] F. E. Van Beek, W. M. B. Tiest, W. Mugge, and A. M. Kappers, "Haptic perception of force magnitude and its relation to postural arm dynamics in 3D," *Scientific Reports*, vol. 5, no. 1, pp. 1–11, 2015.
- [20] M. Jorda, R. Balachandran, J. H. Ryu, and O. Khatib, "New passivity observers for improved robot force control," in *IEEE International Conference on Intelligent Robots and Systems*, 2017, pp. 2177–2184.
- [21] R. Balachandran, M. Jorda, J. Artigas, J. H. Ryu, and O. Khatib, "Passivity-based stability in explicit force control of robots," in *IEEE International Conference on Robotics and Automation*, 2017, pp. 386–393.
- [22] D. P. Kingma and J. Ba, "Adam: A method for stochastic optimization," presented at the 3rd International Conference on Learning Representations, 2015, arXiv:1412.6980.
- [23] Y. Kim and F. Lewis, "Neural network output feedback control of robot manipulators," *IEEE Transactions on Robotics and Automation*, vol. 15, no. 2, pp. 301–309, 1999.
- [24] T. Hayakawa, W. M. Haddad, and N. Hovakimyan, "Neural network adaptive control for a class of nonlinear uncertain dynamical systems with asymptotic stability guarantees," *IEEE Transactions on Neural Networks*, vol. 19, no. 1, pp. 80–89, 2008.
- [25] J. Colgate and J. Brown, "Factors affecting the z-width of a haptic display," in *IEEE International Conference on Robotics and Automation*, 1994, pp. 3205–3210.
- [26] D. Galeazzi, A. Mariani, S. Sahu, S. Maglio, E. De Momi, S. Tognarelli, and A. Menciassi, "A sensorized physical simulator for training in robot-assisted lung lobectomy," presented at the Hamlyn Symposium on Medical Robotics, 2021.